Bone 67 (2014) 257–268

Contents lists available at ScienceDirect

Bone

journal homepage: www.elsevier.com/locate/bone

Original Full Length Article

Effect of sequential treatments with alendronate, parathyroid hormone (1–34) and raloxifene on cortical bone mass and strength in ovariectomized rats☆

Sarah K. Amugongo [a,1], Wei Yao [a,1], Junjing Jia [a], Weiwei Dai [a], Yu-An E. Lay [a], Li Jiang [a], Danielle Harvey [b], Elizabeth A. Zimmermann [c], Eric Schaible [d], Neil Dave [c], Robert O. Ritchie [a,e], Donald B. Kimmel [f], Nancy E. Lane [a,*]

[a] Musculoskeletal Research Unit, Department of Medicine, University of California Davis Medical Center, Sacramento, CA 95817, USA
[b] Division of Biostatistics, Department of Public Health Sciences, University of California, Davis, CA 95616, USA
[c] Materials Sciences Division, Lawrence Berkeley National Laboratory, Berkeley, CA 94720, USA
[d] Experimental Systems Group, Advanced Light Source, Lawrence Berkeley National Laboratory, Berkeley, CA 94720, USA
[e] Department of Materials Science and Engineering, University of California, Berkeley, CA 94720, USA
[f] Osteoporosis Research Center, School of Medicine, Creighton University, Omaha, NE 68131, USA

ARTICLE INFO

Article history:
Received 11 January 2014
Revised 3 April 2014
Accepted 16 April 2014
Available online 10 July 2014

Edited by: David Burr

Keywords:
Adult
Mineralization
MicroCT
Lamellar bone
Mineralizing surface
Indentation

ABSTRACT

Anti-resorptive and anabolic agents are often prescribed for the treatment of osteoporosis continuously or sequentially for many years. However their impact on cortical bone quality and bone strength is not clear.
Methods: Six-month old female rats were either sham operated or ovariectomized (OVX). OVX rats were left untreated for two months and then were treated with vehicle (Veh), hPTH (1–34) (PTH), alendronate (Aln), or raloxifene (Ral) sequentially for three month intervals, for a total of three periods. Mid-tibial cortical bone architecture, mass, mineralization, and strength were measured on necropsy samples obtained after each period. Bone indentation properties were measured on proximal femur necropsy samples.
Results: Eight or more months of estrogen deficiency in rats resulted in decreased cortical bone area and thickness. Treatment with PTH for 3 months caused the deposition of endocortical lamellar bone that increased cortical bone area, thickness, and strength. These improvements were lost when PTH was withdrawn without followup treatment, but were maintained for the maximum times tested, six months with Ral and three months with Aln. Pre-treatment with anti-resorptives was also somewhat successful in ultimately preserving the additional endocortical lamellar bone formed under PTH treatment. These treatments did not affect bone indentation properties.
Summary: Sequential therapy that involved both PTH and anti-resorptive agents was required to achieve lasting improvements in cortical area, thickness, and strength in OVX rats. Anti-resorptive therapy, either prior to or following PTH, was required to preserve gains attributable to an anabolic agent.

Introduction

Musculoskeletal diseases including osteoporosis are the second greatest cause of disability worldwide. Their overall impact on death and disability has increased 45% over the past 20 years [1,2]. Treatments for osteoporosis now focus on two major medication classes, anti-resorptive and anabolic agents. All the approved anti-resorptive agents for the treatment of osteoporosis, that include selective estrogen receptor modulators (SERMs), an inhibitor of RANKL, and bisphosphonates, preserve bone mass and strength by suppressing bone turnover. Most preclinical studies with these bone active agents only evaluate their effects on trabecular bone [3–5,75]. All preserve trabecular bone mass, microarchitecture and bone strength. Numerous clinical trials have demonstrated that these agents reduce the risk of vertebral fractures in

Abbreviations: AED, average energy dissipation (J); Aln, alendronate (Sigma, Cat# A-4978, St. Louis, MO, USA); BMU, basic multicellular unit; DBM, degree of bone mineralization (microCT); IDI, first cycle indentation distance (IDI) (μm); PTH, parathyroid hormone [hPTH (1–34) (human) acetate (Bachem Biosciences Inc., Cat# H-4835, King of Prussia, PA USA)]; Ral, raloxifene (Sigma, Cat# R-1402, St. Louis, MO, USA); Veh, normal saline (Life Technologies, Cat# 10010, Grand Island, NY, USA).

☆ This work was funded by National Institutes of Health (NIH) Grant #s R01 AR043052 and 5K24AR048841. The statistical analyses were supported by the National Center for Advancing Translational Sciences (NCATS), and NIH, through Grant #UL1 TR000002. The involvement of ROR was supported by the National Institutes of Health (NIH/NIDCR) under Grant# 5R01 DE015633 to the Lawrence Berkeley National Laboratory (LBNL).

* Corresponding author at: Endowed Professor of Medicine and Rheumatology, Director, Center for Musculoskeletal Health, 4625 2nd Avenue, Suite 1002, Sacramento, CA 95817, USA. Fax: +1 916 734 4773.
E-mail address: nelane@ucdavis.edu (N.E. Lane).
[1] These authors contributed equally to the study.

http://dx.doi.org/10.1016/j.bone.2014.04.033
8756-3282/

women with established osteoporosis [6–14]. Alendronate, denosumab, and zoledronic acid also reduce incident hip fracture risk [15,16]. PTH (1–34), the sole approved anabolic agent, stimulates bone formation, increases bone mass and bone strength, and improves trabecular microarchitecture in preclinical studies [17–19]. It also decreases the risk of both vertebral and non-vertebral fragility fractures in osteoporotic humans [20–23].

The effects of anti-resorptive agents and PTH (1–34) on trabecular bone in animal models and osteoporotic patients are well-known [24]. One short duration study in intact rats not only reported that PTH had greater effects on cancellous bone than cortical bone, but also suggested that it might be more efficacious in intact rats than in rats with low bone mass [25]. This intriguing finding deserves longer-term followup. Preclinical data suggest that PTH may either decrease or increase the degree of bone mineralization (DBM) of cortical bone [22,26]. Results from clinical study samples found that PTH decreases DBM [27]. Similarly, raloxifene, a selective estrogen receptor modulator, reduces vertebral fracture risk in postmenopausal osteoporotic women despite very modest bone turnover suppression and gain in lumbar spine bone mineral density (BMD) [6,28]. On the other hand, bisphosphonates decrease fracture risk, increase BMD, reduce activation frequency, increase DBM [29–36], and may be associated with improved bone balance at the BMU level [37].

Cortical bone is important because it represents more than 80% of the bone mineral in the human body. It is also difficult to study, because either 3D imaging or histologic techniques must be employed to separate it from the trabecular bone that it surrounds. Moreover, both clinical and pre-clinical data suggest that osteoporosis treatment medications influence cortical bone. Bisphosphonates reduce endocortical bone formation [38,39], Haversian remodeling [39,40] and cortical porosity [35,41–46]; mildly increase cortical thickness [47,48] and increase cortical area [49]; improve cortical bone strength [47]; and have no effect on periosteal bone formation [50]. Bisphosphonates also reduce incident fractures in the proximal femur, a region composed primarily of cortical bone [16,29–36,38]. They may reduce cortical bone fracture risk by changing bone material properties independently of BMD or bone micro- or macroarchitecture [6,31,35,51–54]. Previously we reported that bisphosphonates increase DBM and reduce the heterogeneity of the trabecular bone matrix [54,55]. However, it is not known if the increase in DBM with bisphosphonates is associated with improved cortical bone strength. On the other hand, PTH increases endocortical bone formation [56–61] and cortical porosity [57,58,62,63]; increases cortical area and thickness [19,56,58,61,64–67]; decreases cortical bone strength [62]; increases the rate of Haversian remodeling [58,60,62,65]; and stimulates periosteal bone formation [55,58,59]. The opposite effects of bisphosphonates and PTH on cortical bone endpoints such as cortical porosity and endocortical bone formation rate suggest that combining them in strategic sequences could produce better therapeutic results than can be achieved by any monotherapy.

Osteoporosis patients now routinely cycle through bone active medications [68–72]. It is extremely difficult to do direct studies of fracture risk associated with such sequential treatments in humans, because of the large sample sizes required. Pre-clinical data addressing how these sequential osteoporosis therapies affect cortical bone strength and its surrogate measures could be very helpful. The goal of this study is to determine the effects of sequential treatments with currently approved osteoporosis medications that act through complementary tissue level mechanisms of action, on cortical bone strength and its surrogate measures. We evaluated cortical bone strength, architecture, indentation properties, and estimated strength, in adult ovariectomized (OVX) rats with low bone mass, given various sequences of anti-resorptive and anabolic therapy that have already been or could be applied clinically. We hypothesized that sequential treatment by traditional osteoporosis therapies with complementary tissue level mechanisms of action would improve cortical bone strength in OVX rats.

Methods

Animals and experimental procedures

Six-month-old virgin female Sprague–Dawley rats were purchased from Harlan Laboratories (Livermore, CA, USA). They were either ovariectomized (OVX) or sham-OVXd at the vendor and shipped to our laboratory two weeks post-surgery. They were individually-housed and maintained on rodent chow (Rodent Diet, Cat# 2918, Teklad; Madison, WI, USA) at 21 °C with a 12-hour light/dark cycle. Pair-feeding of OVX to Sham rats was initiated immediately upon arrival. A Sham–OVX ($n = 12$) and an OVX ($n = 10$) group were necropsied at two months post-surgery (Period 0) (Table 1). All remaining OVX rats were then randomized by body weight into ten groups (Table 1) that represented currently-applied and potential sequences of anti-osteoporosis medications.

The groups of OVX rats were treated for three months (Period 1) with Veh (1 ml/kg/dose, 3×/wk by subcutaneous (SC) injection); PTH (25 μg/kg/dose, 5×/wk SC); Aln (25 μg/kg/dose, 2×/wk SC); or Ral (5 mg/kg/dose 3×/wk by oral gavage (Table 1)). No Ral vehicle oral dosing was done. The PTH dose was based on previous publications [25,73,74]; the justification for doses of all drugs is discussed in more detail elsewhere [75]. Each rat was given dual fluorochrome labeling before necropsy by subcutaneous injection. The sequence was calcein (10 mg/kg) on Day 14 followed by alizarin red (20 mg/kg) on Day 4 before necropsy. The study protocol was approved by the University of California Davis Institutional Animal Care and Use Committee.

After 90 days (Period 1), 6–12 animals were randomly-selected from each group and necropsied (Table 1), while the remaining animals were switched to their Period 2 treatment regimen. After 180 days (Period 2), another 10–12 animals from each group were necropsied (Table 1), while the remaining animals were switched to their Period 3 treatment regimen. After 270 days (Period 3), all remaining rats were necropsied ($n = 7$–15/group) (Table 1). During the study, nine rats, randomly-disbursed over the ten groups, died, leaving 383 that reached necropsy as scheduled.

At necropsy, the rats were euthanized by CO_2 inhalation. The uterus was inspected visually to confirm OVX efficacy. Uteri with markedly shrunken horns, including decreased vascularity, yellow/beige color, and reduced diameter and length, were a sign of successful OVX. Both tibiae and femurs and lumbar vertebrae (LV) 5–6 were excised and cleaned. LV5 and LV6 were separated from one another. The right femur, right tibia, and LV5 were placed in 10% formalin for 24 h, then transferred to 70% ethanol for longer-term storage. LV6, the left femur, and the left tibia were wrapped in saline-soaked gauze and frozen at −20 °C until analysis. The data from LV5 and LV6 are reported elsewhere [75].

Biomechanical testing (left tibia)

Testing was performed after 5 mm of the end of each bone had been removed with a low speed saw with a wafering blade 60-20090 (Allied High Tech Products, Rancho Dominguez, CA), to decrease the possibility of buckling during the testing. The tibial test specimens were soaked in 37 °C HBSS (Hanks' Balanced Salt Solution; Sigma) for 12 h prior to testing. Each specimen was subjected to a three-point bending test, with a major loading span of 14.5 mm; the bone was loaded such that the posterior surface was under tension and the anterior surface was under compression, using an EnduraTEC Electro Force 3200 Testing System (Bose Corp., Eden Prairie, MN). Each tibia was loaded to failure at a displacement rate of 0.01 mm/s, and the load and displacement measured, the former using a calibrated 225 N load cell. After testing, a two-point average of the diameter and a six-point average of the cortical shell thickness were measured at the fracture site of each tibia using digital calipers with a 0.01 mm readout. The peak load (N) was recorded from the maximum load in each test. The corresponding yield and

Table 1
Experimental groups.

Treatment group	Period 0 (Days [−60]–0)	Period 1 (Days 1–90)	Period 2 (Days 91–180)	Period 3 (Days 181–270)
Sham	No treatment (12)	No treatment (12)	No treatment (12)	No treatment (7)
OVX				
Veh–Veh–Veh	No treatment (10)	Vehicle (10)	Vehicle (10)	Vehicle (10)
Aln–Aln–Aln		Alendronate (12)	Alendronate (12)	Alendronate (12)
Ral–Ral–Ral		Raloxifene (11)	Raloxifene (11)	Raloxifene (12)
Aln–Veh–Aln		Alendronate (12)	Vehicle (12)	Alendronate (15)
PTH–Veh–Veh		hPTH (1–34) (12)	Vehicle (11)	Vehicle (12)
PTH–Aln–Veh		hPTH (1–34) (12)	Alendronate (12)	Vehicle (11)
PTH–Ral–Ral		hPTH (1–34) (6)	Raloxifene (12)	Raloxifene (12)
Aln–PTH–Veh		Alendronate (12)	hPTH (1–34) (12)	Vehicle (12)
Aln–PTH–Aln		Alendronate (11)	hPTH (1–34) (12)	Alendronate (10)
Ral–PTH–Ral		–	hPTH (1–34) (11)	Raloxifene (11)

Day −60 = day of ovariectomy (OVX). Day 1 = first day of dosing. Period 0 (Day −60 to Day 0) allowed establishment of mild-moderate estrogen-deficiency-related low bone mass. The number of rats necropsied at the end of each period from each group is shown (#). Since Ral treatment during Period 1 was common to the Ral–Ral–Ral and Ral–PTH–Ral groups, no Ral–PTH–Ral rats were necropsied at the end of Period 1.
The treatment regimens were: Vehicle (Veh) subcutaneously (SC) at 1 ml/kg/dose 3×/wk; parathyroid hormone [hPTH (1–34)] (PTH) SC @ 25 μg/kg/dose 5×/wk; alendronate (Aln) SC @ 25 μg/kg/dose 2×/wk; and Raloxifene (Ral) by oral gavage @ 5 mg/kg/dose 3×/wk. No group was orally gavaged to match the Ral groups.

ultimate strengths of the central tibiae (σ) were calculated, in units of Pa, from the standard equation for a beam in three-point bending:

$$\sigma = \frac{PLy}{4I}$$

where respectively, P is the load at yielding (*i.e.*, at the onset of inelastic deformation) or the maximum load reached during the bending test; *L* is the major span between the loading support pins; *y* is the distance from the center of mass; and *I* is the moment of inertia of the cross-section. In addition, toughness (work to failure) was calculated from the load–displacement curve as the work to fracture (energy absorption), and W_f, defined (in units of kJ/m^2) as the area under the load–displacement curve divided by twice the projected area of the fracture surface [76–78]. All tests were done blinded.

Bone histomorphometric measurements

Bone histomorphometric measures were obtained from the right tibial shaft. Nomenclature was applied according to established standards [79]. A 5 mm long specimen that began 1 mm distal to the tibial–fibular junction (TFJ) and extended 4 mm proximal to the TFJ was prepared from each right tibia with an Isomet Saw 1000 (Buehler; Lake Bluff, IL). Each 5 mm specimen was dehydrated and embedded undecalcified in methylmethacrylate and then cross-sectioned using a SP1600 microtome (Leica; Buffalo Grove, IL) into 40 μm sections. The section located 2 mm proximal to the TFJ was analyzed with fluorescent microscopy using image analysis software (Bioquant Image Analysis Corporation; Nashville, TN) for single- and double-labeled perimeters (sL.Pm and dL.Pm) and bone perimeter (B.Pm) at the endocortical surface. Mineralizing surface (Md.Pm/B.Pm) was calculated as (dL.Pm + (sL.Pm / 2)) / B.Pm. Cortical area (Ct.Ar) and the area of lamellar bone applied to the endocortical surface (Ec.Lm.B.Ar) were measured using Osteomeasure (v2, Atlanta, GA, USA). Ec.Lm.B.Ar was expressed both as an absolute value and as a percentage of Ct.Ar. A qualitative evaluation of the periosteal surface for labeling was carried out at the same time.

Cortical bone architecture and degree of mineralization (DBM)

Ex vivo microCT scans were obtained from the central right femur. The scan region began 3 mm proximal to the mid-point of the bone and ended 3 mm distal to its mid-point. The region was scanned at 70 kVp and 85 μA, with a voxel size of 10.5 μm in all three spatial dimensions. 95 consecutive slices at the mid-point were used to evaluate total area (Tt.Ar), cortical area (Ct.Ar), marrow area (Ma.Ar), cortical thickness (Ct.Th), and DBM [22,55].

Surface reference point indentation

Surface reference point indentation measurements were made *ex vivo* on blind-coded, randomized whole right femurs, using established protocols [80–84] modified as noted below. The bone was soaked in normal saline at room temperature for at least 30 min. A 2 mm wide sampling region located 9–18 mm distal to the proximal-most aspect of the greater trochanter and centered on the anterior periosteal surface of the femur, was selected. The periosteum was gently removed with a scalpel. The femur was next oriented anterior surface up, with the center rod of the Ex-Vivo Bone Stage (Biodent™; Active Life Science, Inc.; Santa Barbara, CA), perpendicular to the long axis of the bone. The first test site was 10 mm distal to the proximal-most aspect of the greater trochanter. At each test site, the probe tip was first lowered until it rested on the bone surface. Then, ten load-controlled indents were applied with a 5 N force. Data as listed below were recorded from each site. Several drops of normal saline were applied to the sampling region every 5 min during testing. Up to seven additional test sites located 1 mm apart and 1–7 mm distal to the first site were interrogated as necessary, to achieve five successful measured sites. Only sites in which all ten measurements displayed a touchdown distance of 70–90 μm, and an indentation force of 4.9–5.1 N were accepted. The number of rejected test sites per bone ranged from zero to three. The endpoints measured at successful sites were first cycle indentation distance (IDI) (μm) and AED (average energy dissipation (J)) [80–84]. Both IDI and AED were the average of the values measured at the five separate successful measurement sites.

Finite element modeling (LV5)

We used a μCT-based finite-element model (FEM) to estimate both the maximum load of the whole LV5 and the separate maximum loads of both the cortical shell and the trabecular core. The model simulated uniaxial vertebral compression loading with the cranial and caudal ends fixed between two loading planes. Cortical and trabecular bone regions were segmented by manually tracing the endocortical surface of the cortex for every 15 slices from each scan of 2.2 mm obtained from the central vertebral body, where trabecular bone mass and architectural parameters were evaluated [75]. 3D μCT images of LV5 (10.5 μm voxel resolution) were incorporated into the model [85]. All 3D image voxels were converted to elements. Each FEM mesh had ~9–18 million elements. Each element segmented as bone was assigned a Young's modulus of 18 GPa and a Poisson ratio of 0.3 [86]. Details of the numerical method have been published [87,88]. The boundary

conditions that defined the load platen–specimen interface were assumed to be frictionless. Total strength and the load-carrying capacity of the vertebral trabecular bone were calculated from finite-element analyses, as previously [54,72,89].

Statistics

Primary analysis for key measures of bone strength, bone histomorphometry, bone architecture and mineralization, reference point indentation, and LV5 finite element analysis assessed differences among groups after the full course of treatment (Period 3). Values more than 2.5 standard deviations away from the mean of each group were removed as outliers. Analysis of variance (ANOVA) was performed separately for each endpoint. If the global test for a difference among groups was significant ($P < 0.001$, more strict due to multiple comparisons), post-hoc pairwise comparisons were made between the Veh–Veh–Veh and the nine treatment groups (all pairwise comparisons including between treatment groups) using Tukey's Honestly Significant Difference approach to multiple comparison adjustment. A separate comparison was made between Sham and Veh–Veh–Veh. Only differences that remained significant after the multiple comparison adjustment are reported. Secondary analyses used the same approach on the Period 0 (comparing Sham and OVX), Period 1, and Period 2 values, separately at each time point for these endpoints.

Predictors of maximum load for all central tibiae from all time periods were studied by multiple regression analysis of cortical thickness, cortical area, and degree of mineralization. Bone strength estimated by FEA was correlated to whole bone strength measured in LV6 by linear regression [75].

For a subset of five key endpoints, a trajectory analysis was performed using linear regression models and all data from all groups and periods. This analysis assumed that the values in the Sham rats did not change over time (which was checked and supported by the data), but that OVX rats may experience change over time. The models then assessed three key questions: 1) does active treatment modify the trajectory and does it vary by treatment type; 2) does switching from an active treatment to vehicle contribute to the measurements and does that differ by active treatment; and 3) is there a "salvage" effect by switching from vehicle back to active treatment. The model further assumed that the order of the therapy did not matter, so that the average measurement at a given time point was a cumulative impact of the therapeutic experience up to that time. Variables for each group and each period where then constructed to reflect time on a specific active treatment, time on vehicle after being on a specific active treatment, and time back on treatment after being on vehicle. For example, at Period 2, animals in the PTH–Aln–Veh group would have a contribution of PTH for three months and a contribution of Aln for three months, while at Period 3, rats in that group would have a contribution of PTH for three months, Aln for three months, and switching from Aln to vehicle and therefore being off Aln for three months. Results describe the average impact of being on a particular treatment, switching from a specific treatment to no treatment, or switching from no treatment to a treatment. In the trajectory analyses, a P-value < 0.05 was considered statistically significant.

All analyses were performed using SAS v9.2 (Cary, NC, USA).

Results

At necropsy, all rats that underwent OVX surgery displayed uterine atrophy, indicating successful OVX. Similarly, no uteri of Sham-OVX rats showed signs of atrophy.

Bone strength

Period 3

Central tibia maximum load (Table 2) was affected by neither estrogen status, nor traditional osteoporosis monotherapy, as represented by Aln–Aln–Aln, Ral–Ral–Ral, and PTH–Veh–Veh. Maximum load was significantly better in Aln–Veh–Aln than in Veh–Veh–Veh rats. Maximum load was also significantly better than Veh–Veh–Veh in all groups that received both PTH and Aln at some time during the experiment (Table 2). In contrast, maximum stress was affected by neither estrogen status, nor any applied treatment. Work to failure was not affected by estrogen status and was significantly different from Veh–Veh–Veh only in the Aln–Veh–Aln and Ral–PTH–Ral groups.

Other times

At the end of Period 0, no bone strength endpoints were affected by estrogen status (Supplementary Table 1).

At the end of Period 1, maximum load was lower in Sham than in Veh–Veh–Veh rats and lower in Ral–Ral–Ral rats than in all other groups except Aln–Aln–Aln. Neither maximum stress nor work to failure was affected by estrogen status or any treatment (Supplementary Table 2).

At the end of Period 2, maximum load was not affected by estrogen deficiency and was significantly higher in Aln–Veh–Aln, PTH–Aln–Veh, PTH–Ral–Ral, Aln–PTH–Veh, and Aln–PTH–Aln rats than in Veh–Veh–Veh and Ral–Ral–Ral. Neither maximum stress nor work to failure was affected by estrogen status or any treatment (Supplementary Table 3).

Predictors of bone strength

Cortical area accounted for the largest percentage of the variability in central tibia maximum load ($R^2 = 0.4521$, $P < .0001$). When cortical thickness was added to the model, it accounted for an additional 3.06% of the variability. Together they accounted for nearly half the variation in bone strength ($R^2 = 0.4827$, $P < .0001$). Degree of bone mineralization was not associated with central tibia maximum load.

Bone histomorphometry

Qualitative examination of the periosteal surfaces for fluorochrome label revealed little label and no trends of any sort.

Period 3

Ec.Md.Pm/B.Pm. was higher in PTH–Veh–Veh than in Aln–Aln–Aln, PTH–Aln–Veh, PTH–Ral–Ral, and Aln–PTH–Aln. PTH–Ral–Ral was significantly lower than Veh–Veh–Veh, while all others displayed no significant difference from Veh–Veh–Veh (Table 2).

About 1% of cortical bone was composed of endocortical lamellar bone in Veh–Veh–Veh rats. There was no significant difference between PTH–Veh–Veh and Veh–Veh–Veh rats. However, all rats treated with PTH at one time and anti-resorptive therapy at another time, except for PTH–Ral–Ral, had significantly more endocortical lamellar bone than either Veh–Veh–Veh or PTH–Veh–Veh (Table 2).

Other times

At the end of Period 0, there were no significant differences between Veh–Veh–Veh and Sham rats (Supplementary Table 1).

At the end of Period 1, Ec.Md.Pm/B.Pm. was not affected by estrogen status and no groups differed from Veh–Veh–Veh. However, Aln–Veh–Aln rats had significantly lower Ec.Md.Pm/B.Pm. than all groups besides Aln–Aln–Aln and Ral–Ral–Ral. Aln–Aln–Aln rats were also significantly lower than PTH–Veh–Veh and Aln–PTH–Aln. About 1% of cortical bone was composed of endocortical lamellar bone in Veh–Veh–Veh rats. PTH–Veh–Veh and PTH–Aln–Veh had approximately five times as much endocortical lamellar bone as Veh–Veh–Veh rats (Supplementary Table 2).

At the end of Period 2, Ec.Md.Pm/B.Pm. was higher in Veh–Veh–Veh than in Sham rats. It was lower in Aln–Aln–Aln, PTH–Veh–Veh, PTH–Aln–Veh rats than in Veh–Veh–Veh rats and higher in Aln–PTH–Aln rats than in Veh–Veh–Veh rats (Supplementary Table 3).

At the end of Period 2, about 0.6% of cortical bone was composed of endocortical lamellar bone in Veh–Veh–Veh rats. PTH–Veh–Veh and PTH–Ral–Ral had the same amount of endocortical lamellar bone as

Table 2
Values at close of Period 3 (Day 270 — end of experiment).

Endpoint	Units	Sham (s)	Veh–Veh–Veh (o)	Aln–Aln–Aln (a)	Ral–Ral–Ral (b)	Aln–Veh–Aln (c)	PTH–Veh–Veh (d)	PTH–Aln–Veh (e)	PTH–Ral–Ral (f)	Aln–PTH–Veh (g)	Aln–PTH–Aln (h)	Ral–PTH–Ral (i)
Central tibia												
Max load	N	104.8 ± 23.5	92.3 ± 9.5	104.8 ± 13.0^{c}	102.7 ± 8.2^{c}	119.1 ± 9.1^{d,f,o}	103.4 ± 11.6^{c}	110.4 ± 10.5^{o}	105.9 ± 8.7^{o}	115.0 ± 6.3^{o}	115.6 ± 9.0^{o}	114.8 ± 10.2^{o}
Max stress	N/mm^2	156.5 ± 36.0	137.7 ± 23.4	147.2 ± 27.3	150.9 ± 16.8	154.4 ± 17.5	140.1 ± 24.0	150.5 ± 34.2	140.4 ± 16.9	153.5 ± 12.0	157.7 ± 23.7	164.6 ± 21.6
Work to failure	kJ/mm^2	2.13 ± 0.97	1.65 ± 0.35	2.07 ± 0.84	2.35 ± 0.56	2.75 ± 0.53^{d,f,o}	1.82 ± 0.66	2.18 ± 0.62	2.07 ± 0.35	2.42 ± 0.45	2.34 ± 0.51	2.50 ± 0.49^{o}
Ec.Md.Pm/B.Pm	%	0.66 ± 0.30	0.67 ± 0.29	0.31 ± 0.16^{d}	0.64 ± 0.30^{f}	0.70 ± 0.26^{f}	0.98 ± 0.42^{e,f,h}	0.29 ± 0.24	0.19 ± 0.14^{o}	0.56 ± 0.37	0.39 ± 0.19	0.51 ± 0.50
Ec.Lm.B.Ar	mm^2	–	0.024 ± 0.029	–	–	–	0.034 ± 0.050^{e,g,h,i}	0.146 ± 0.078^{o}	0.095 ± 0.062^{i}	0.161 ± 0.098^{o}	0.194 ± 0.045^{o}	0.206 ± 0.094^{o}
Lamellar (as % of Ct.Ar)	%	–	1.01 ± 1.19	–	–	–	0.67 ± 0.77^{e,g,h,i}	4.02 ± 2.01^{o}	2.64 ± 1.63^{i}	4.92 ± 3.05^{o}	5.37 ± 1.10^{o}	5.42 ± 2.39^{o}
Tt.Ar	mm^2	10.48 ± 0.61	10.48 ± 0.50	11.18 ± 0.80	10.77 ± 0.70	11.31 ± 0.64	10.89 ± 0.66	10.68 ± 0.64	10.54 ± 0.40	10.89 ± 0.73	10.94 ± 0.69	10.87 ± 0.99
Ct.Ar	mm^2	7.00 ± 0.39^{o}	6.19 ± 0.44	7.72 ± 0.32^{b,d,o}	6.37 ± 0.50^{c,e,f,g,h,i}	7.75 ± 0.49^{d,o}	6.59 ± 0.50^{e,g,h,i}	7.65 ± 0.56^{o}	7.14 ± 0.44^{h,o}	7.59 ± 0.45^{o}	8.03 ± 0.52^{o}	7.75 ± 0.79^{o}
Ma.Ar	mm^2	3.42 ± 0.47^{o}	3.01 ± 0.38	3.19 ± 0.38^{b,d,e}	4.21 ± 0.36^{c,f,g,h,i,o}	3.52 ± 0.25^{d,e}	4.31 ± 0.44^{f,g,h,i,o}	4.11 ± 0.63^{f,g,h,i,o}	3.44 ± 0.22	3.45 ± 0.49	3.36 ± 0.39	2.93 ± 0.45
Ct.Th	mm	0.733 ± 0.048^{o}	0.648 ± 0.057	0.717 ± 0.047	0.705 ± 0.024^{c}	0.779 ± 0.067^{d,o}	0.662 ± 0.067^{e,f,h,i}	0.739 ± 0.042^{o}	0.754 ± 0.048^{o}	0.744 ± 0.026^{o}	0.779 ± 0.032^{o}	0.798 ± 0.048^{o}
DBM		1121 ± 25.7	1122 ± 18.6	1143 ± 16.5^{b}	1116 ± 13.1^{e,f,g,i}	1131 ± 13.8	1128 ± 23.9	1141 ± 15.9	1142 ± 11.0	1139 ± 12.0	1135 ± 18.3	1140 ± 15.2
Proximal femur												
IDI		10.29 ± 1.28	10.59 ± 1.99	9.31 ± 2.41	9.43 ± 1.26	8.87 ± 2.37	10.25 ± 3.10	9.88 ± 1.86	9.98 ± 1.51	8.91 ± 1.75	10.56 ± 3.20	10.27 ± 2.38
AED		29.92 ± 4.59	25.96 ± 5.71	24.22 ± 4.42	22.82 ± 4.06	21.30 ± 2.70	21.95 ± 4.32	20.94 ± 2.87	24.98 ± 7.26	25.22 ± 3.86	26.86 ± 7.66	25.23 ± 5.37
Vertebral body												
Estimated failure load	N	162 ± 24^{o}	99 ± 17	148 ± 14^{b,d,e,h,o}	122 ± 16^{c,d,e,g,h,i}	162 ± 20^{d,f,h,o}	97 ± 12^{e,f,g,h,i}	176 ± 15^{d,f,o}	138 ± 19^{g,h,o}	163 ± 12^{h,o}	202 ± 25^{i,o}	153 ± 19^{o}
%load carried by Ct bone	%	47.6 ± 16.1	60.4 ± 9.1	52.6 ± 9.5	45.5 ± 12.9^{o}	54.3 ± 12.6	52.6 ± 12.5	40.8 ± 11.6^{o}	48.4 ± 9.8	51.1 ± 7.9	51.5 ± 8.6	45.5 ± 6.1

Mean ± SD.
Groups are identified by letters a–i and o; superscripts denote differences from groups to right. All groups are labeled "o" when different from Veh–Veh–Veh.
Ec.Lm.B.Ar = endocortical lamellar bone area.
Ec.Md.Pm/B.Pm = endocortical mineralizing surface.
A total of 8 observations were identified as outliers and excluded from the analyses: 1) one from the PTH–Ral–Ral group in the analysis of Ec.MS/BS; 2) one from the PTH–Veh–Veh group in the analysis of lamellar (as % of Ct.Ar); 3) one from the Aln–Aln–Aln group in the analysis of Ct.Ar; 4) one from the PTH–Aln–Veh group in the analysis of Ct.Th; 5) one from the Aln–Aln–Aln group in the analysis of AED; 6) one from the Ral–PTH–Ral in the analysis of estimated failure load; 7) one from the Aln–Veh–Aln in the analysis of estimated failure load; 8) one from the Aln–Veh–Aln group in the analysis of %load carried by Ct bone.

Veh–Veh–Veh rats. However, PTH–Aln–Veh, Aln–PTH–Veh, Aln–PTH–Aln, and Ral–PTH–Ral had significantly more endocortical lamellar bone than Veh–Veh–Veh rats, showing 5.6–6.7% of Ct.Ar as endocortical lamellar bone (Supplementary Table 3).

Bone architecture and mineralization

Period 3

Total area was not influenced by estrogen status or any treatment. Cortical area was significantly higher in Sham, Aln–Aln–Aln, and Aln–Veh–Aln rats than in Veh–Veh–Veh rats. Cortical area was also significantly higher in rats that received both anti-resorptive and formation stimulation therapies at some point, and was significantly higher in those groups, except for PTH–Ral–Ral, than in Ral–Ral–Ral and PTH–Veh–Veh (Table 2). Marrow area was significantly higher in Ral–Ral–Ral, PTH–Veh–Veh, and PTH–Aln–Veh rats than in Veh–Veh–Veh rats (Table 2).

Cortical thickness was significantly greater in Sham, Aln–Veh–Aln, and PTH–Ral–Ral than in Veh–Veh–Veh. Neither Ral–Ral–Ral nor PTH–Veh–Veh differed significantly from Veh–Veh–Veh. Cortical thickness was significantly better in all groups that received both PTH and Aln at some time during the experiment than in Veh–Veh–Veh rats. Interposing PTH treatment in the midst of either Aln or Ral treatment caused a significant improvement in cortical thickness (Table 2).

DBM was not influenced by estrogen status, but was significantly higher in groups that received both anti-resorptive and formation stimulation therapies than in Ral–Ral–Ral (Table 2).

Other times

At the end of Period 0, marrow area was significantly higher in Veh–Veh–Veh than in Sham rats. However, cortical thickness and DBM were the same in Veh–Veh–Veh and Sham rats (Supplementary Table 1).

At the end of Period 1, total area did not differ with estrogen deficiency or among the treatment groups. Cortical area was significantly higher in PTH–Veh–Veh, PTH–Aln–Veh, Aln–PTH–Veh, and Aln–PTH–Aln rats than in Veh–Veh–Veh and Ral–Ral–Ral rats. Marrow area was significantly lower in Aln–Aln–Aln, Aln–Veh–Aln, and PTH–Aln–Veh, rats than in Veh–Veh–Veh rats. Cortical thickness was the same as Veh–Veh–Veh in all groups except PTH–Veh–Veh. DBM was significantly higher in Sham, Aln–PTH–Veh, and Aln–PTH–Aln than in Veh–Veh–Veh rats (Supplementary Table 2).

At the end of Period 2, total area did not differ among the groups. Cortical area was significantly higher in all other groups than in Veh–Veh–Veh and Ral–Ral–Ral. Marrow area was significantly higher than Veh–Veh–Veh in all groups except Aln–Aln–Aln, and Aln–PTH–Aln. Cortical thickness was significantly higher than Veh–Veh–Veh in Sham, Aln–Veh–Aln, Aln–PTH–Veh, Aln–PTH–Aln, and Ral–PTH–Ral rats. DBM was significantly higher than Veh–Veh–Veh in all groups, except Ral–Ral–Ral and PTH–Veh–Veh (Supplementary Table 3).

Reference point indentation

There was no significant effect of estrogen deficiency or any treatment on either IDI or AED at any time (Table 2, Supplementary Tables 1–3).

Finite element analysis of LV5

Estimated failure load in LV5 was well-correlated to actual maximum load in LV6 ($R = 0.709$, $P < .001$), according to the following equation: Estimated Failure Load $= 0.265 * \text{Maximum Load} + 86.5$. The slope, significantly less than 1.00 ($P < .001$), indicated that the current FEM underestimates the strength of stronger bones.

Period 3

Estimated failure load was significantly higher in all groups except Ral–Ral–Ral and PTH–Veh–Veh, than in Veh–Veh–Veh. The highest value occurred in Aln–PTH–Aln, that was significantly greater than all other groups except PTH–Aln–Veh. The percentage of load carried by cortical bone in the vertebral body was 20–25% higher ($P > .05$) in Veh–Veh–Veh than in Sham rats. This shift to cortical bone tended to be reversed with all treatments, significantly so with Ral–Ral–Ral and PTH–Aln–Veh (Table 2).

Other times

At the end of Period 0, estimated failure load was the same in Veh–Veh–Veh and Sham rats. The percentage of load carried by cortical bone in the vertebral body did not differ between the groups (Supplementary Table 1).

At the end of Period 1, estimated failure load was significantly higher in Sham, Aln–Veh–Aln, PTH–Veh–Veh, PTH–Aln–Veh, PTH–Ral–Ral, than in Veh–Veh–Veh. The percentage of load carried by cortical bone in the vertebral body was 25% lower in Aln–Aln–Aln than in Veh–Veh–Veh rats (Supplementary Table 2).

At the end of Period 2, estimated failure load was significantly higher than Veh–Veh–Veh in Sham and all treatment groups except PTH–Veh–Veh. The highest values occurred in PTH–Aln–Veh, Aln–PTH–Veh, Aln–PTH–Aln, and Ral–PTH–Ral, which were significantly higher than Ral–Ral–Ral and PTH–Ral–Ral. The percentage of load carried by cortical bone was the same in all groups (Supplementary Table 3).

Trajectory analyses

Maximum load

Maximum load decreased in Veh–Veh–Veh rats ($P = 0.04$). Aln increased 1.8 N/month ($P < 0.001$), PTH increased maximum load 4.3 N/month ($P < 0.001$), and Ral does not affect maximum load relative to Veh–Veh–Veh ($P = 0.17$). Maximum load continued to increase when switching from Aln to vehicle ($P = 0.002$), while switching from PTH to vehicle causes maximum load to decrease at the same rate as Veh–Veh–Veh rats. Switching back to Aln from vehicle results in a trend toward increased maximum load ($P = 0.06$).

Work-to-failure (toughness)

Work-to-failure decreased significantly in Veh–Veh–Veh rats ($P = 0.01$). Aln or Ral treatment slows the decline in work-to-failure ($P = 0.03$ or $P = 0.005$, respectively), relative to Veh–Veh–Veh. Treatment with PTH has a greater impact ($P < 0.001$) than either Aln or Ral, relative to Veh–Veh–Veh, showing a slight monthly increase. Switching from Aln to vehicle resulted in an overall increase in work-to failure ($P < 0.001$), but switching from PTH to vehicle causes work-to-failure to decline ($P = 0.76$) at the same rate as Veh–Veh–Veh rats. Returning to Aln from vehicle maintains the work-to-fail change rate at the same level as continuous Aln treatment ($P = 0.14$).

Cortical thickness

Cortical thickness decreased in Veh–Veh–Veh rats ($P < 0.001$). In rats treated with Aln or Ral, cortical thickness decreased more slowly (both $P < .001$) than in Veh–Veh–Veh rats. PTH has a greater impact ($P < 0.001$) relative to Veh–Veh–Veh than either Aln or Ral, resulting in a slight increase. Switching from Aln to vehicle is still superior to Veh–Veh–Veh ($P = 0.01$), resulting in stable cortical thickness. Switching from PTH to vehicle results in a trend for a greater decrease over time than Veh–Veh–Veh ($P = 0.06$). Switching from vehicle back to Aln further slows the rate of loss of cortical thickness compared to Veh–Veh–Veh ($P = 0.05$).

Cortical area

Cortical area decreased in Veh–Veh–Veh rats ($P < 0.001$). Treatment with Aln ($P < 0.001$) or PTH ($P < 0.001$) results in an increase in cortical

area with time. Cortical area also decreased less during Ral treatment than with Veh–Veh–Veh ($P = 0.02$). Switching from Aln to vehicle continues to cause increased cortical area ($P = 0.001$), but switching from PTH to vehicle resulted in a rate of decline similar to that in Veh–Veh–Veh rats ($P = 0.16$). Switching from vehicle back to Aln ($P = 0.41$) did not change the rate of change, still being superior to Veh–Veh–Veh rats.

Endocortical lamellar bone area

Endocortical lamellar bone area is constant in Veh–Veh–Veh rats ($P = 0.88$). Treatment with Aln ($P = 0.30$) or Ral ($P = 0.34$) had no impact on endocortical lamellar bone area. However, treatment with PTH increased endocortical lamellar bone area over time ($P < 0.001$). Switching from PTH to vehicle results in a greater decrease in endocortical lamellar bone area than in Veh–Veh–Veh rats ($P = 0.002$). Switching from Aln to vehicle tends to result in a greater decrease ($P = 0.09$) than in Veh–Veh–Veh rats.

Discussion

We studied cortical bone in adult OVX rats given both traditional monotherapy and sequential therapies with approved agents for human osteoporosis that operate through complementary tissue level mechanisms of action. We administered them during three consecutive three month treatment periods during ages 8–17 months, beginning with OVX rats that had already lost bone and were still losing bone. We measured bone strength and several surrogate measures for bone strength in the central tibia on necropsy samples. For the most part, sequential therapy that involved an anabolic agent showed the best cortical bone strength. We also found that anti-resorptive therapy, either preceding or following PTH, was required to maintain gains caused by PTH (Figs. 2–5).

No traditional monotherapy for osteoporosis had a long-term positive effect on maximum load. For the most part, achieving significant improvement, in the range of 15–29%, compared to untreated OVX rats required sequential treatment with both anti-resorptive and anabolic agents. The only exception was the alendronate "holiday" group (Aln–Veh–Aln), that had better bone strength after six–nine months. Toughness (work-to-failure) was either maintained or occasionally improved, while bone material properties, as reflected by maximum stress, were always maintained. No detrimental effect on either endpoint was ever observed.

PTH stimulated the appearance of an easily-discernible "packet" of endocortical lamellar bone in the central tibia, as previously seen with twice the dose [61,64,66,90,91]. The amount was approximately the same regardless of whether PTH treatment had been preceded by anti-resorptive therapy. When anti-resorptive therapy was applied either before or after PTH treatment, this endocortical lamellar bone was completely maintained by continuous anti-resorptive therapy and partially maintained by intermittent anti-resorptive therapy. When no anti-resorptive therapy was ever applied, the endocortical lamellar bone disappeared within 3–6 months of PTH cessation. The groups in which this lamellar bone was present [61,64,91,92], or partially or fully-maintained, were those in which bone strength was better [61]. It can be deduced by approximation that the average thickness of this lamellar bone was ~30 μm or 3–4% of total cortical thickness in this region. Humans appear to experience such cortical thickening in response to PTH treatment [56,59,93–98]. If a proportional response occurs in cortical bone of humans given PTH, instrumentation such as XTremeCT (high resolution pQCT) with its voxel resolution of 82 μm might have sufficient resolution to detect it [100–102]. The treatment groups that retained this lamellar bone had better maximum load. It is well known that adult rat cortical bone, unlike adult human cortical bone, has no intrinsic Haversian remodeling activity that can be stimulated by this amount of PTH [103]. Our data may also suggest that cortical bone in PTH-treated humans could be temporarily "protected" from

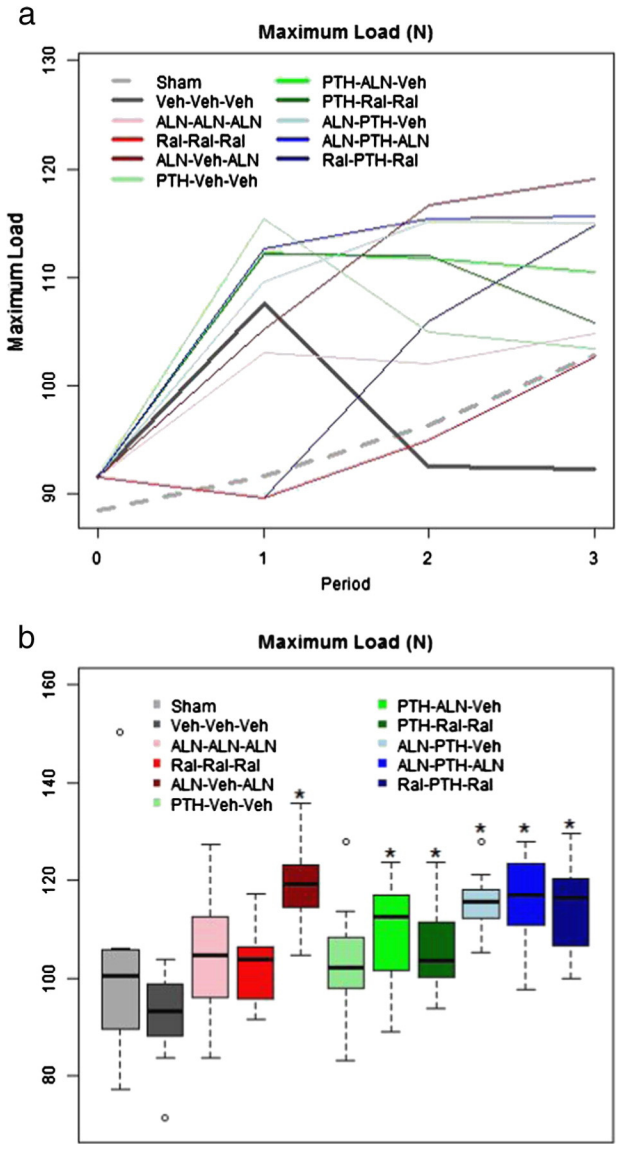

Fig. 1. a. Maximum load by group throughout the study. Treatment with Aln or PTH increased maximum load. Switching from PTH to vehicle results in the same maximum load by the end of the study, as in OVX rats that receive no treatment. Note that OVX and Sham referent groups are depicted by thickened solid or dashed lines, respectively. b. Maximum load at end of study. Boxes are defined by the 25th and 75th percentiles, with the median marked by a solid line inside the box. "Whiskers" of the boxplots extend to the last observation within 1.5× the length of the box (interquartile range) from the edges of the box. Any observed points beyond the whiskers are show as an open circle. Boxes marked with an asterisk are significantly different from the Veh–Veh–Veh group after a Tukey adjustment for multiple comparisons. Except for the Aln "holiday" group, only groups that received both PTH and some combination of pre-PTH or post-PTH anti-resorptive treatment had greater maximum load at the end of the study. Traditional monotherapies produced no significant changes.

activation of Haversian remodeling by prior or concomitant anti-resorptive therapy, making it functionally like rat cortical bone that lacks Haversian remodeling [104]. Therefore, with temporary anti-resorptive protection that prevents the usual increase in cortical porosity, improvement in cortical bone strength in humans might be achieved by PTH treatment that stimulates the deposition of new lamellar bone at the endocortical surface.

Endocortical mineralizing surface (eMd.Pm/B.Pm) in the central tibia was very low, never greater than 1.42%, at the conclusion of PTH treatment. Endocortical Md.Pm/B.Pm (eMd.Pm/B.Pm) was occasionally significantly lower in anti-resorptive treated groups than in untreated

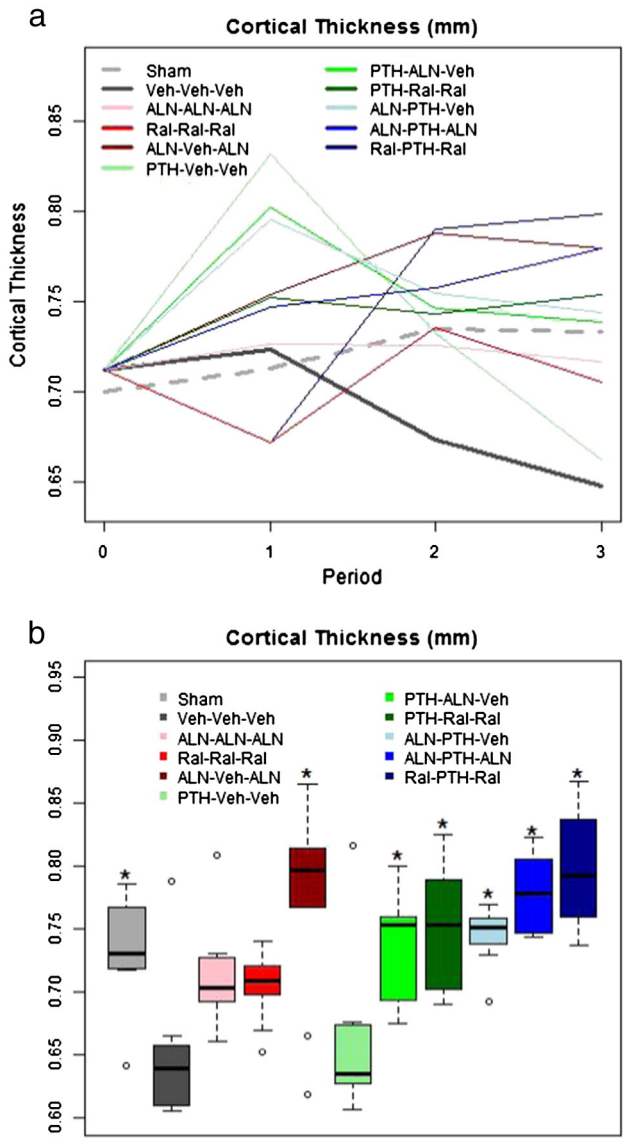

Fig. 2. a. Cortical thickness by group throughout study. Treatment with PTH increases cortical thickness. Note complete loss of PTH-related cortical thickness increase after PTH discontinuation without followup anti-resorptive treatment. The Aln "holiday" group showed improved cortical thickness. b. Cortical thickness at end of study. Boxes are as described in Fig. 1b. Cortical thinning was observed in OVX rats by the end of the study. Except for the Aln "holiday" group, only groups that received both PTH and some combinaton of pre-PTH or post-PTH anti-resorptive treatment had greater cortical thickness than untreated rats at the end of study.

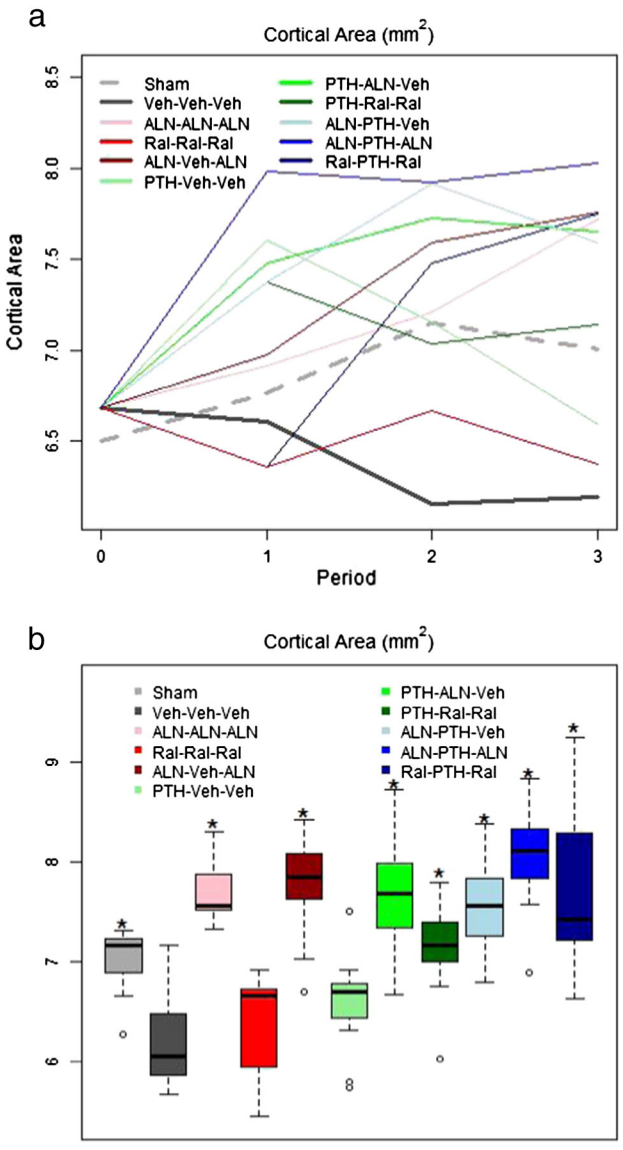

Fig. 3. a. Cortical area by group throughout study. OVX rats experienced a modest decline in cortical area during the study period. Treatment with Aln or PTH increases cortical area, but switching from PTH to vehicle results in a decline similar to rats that never receive treatment. b. Cortical area at end of study. Boxes are as described in Fig. 1b. Reduced cortical area was observed in OVX rats by the end of the study. Except for the Aln "holiday" group, only groups that received both PTH and either pre- or post-PTH anti-resorptive treatment had greater cortical area than untreated rats by the end of study.

rats. It is known that PTH treatment stimulates this endpoint in both rats [61,64,66] and humans [56,58,93–98]. However, it is also known that by 15 wks of treatment, the effect of PTH on eMd.Pm/B.Pm has begun to wane [61]. We suspect that with the relatively modest dose of PTH used in this study and only having data from the 15 wk treatment, we probably have missed the peak PTH stimulation of eMd.Pm/B.Pm that most likely occurred earlier. The presence of endocortical lamellar bone in all PTH-treated rats demonstrates the consistency of the endocortical effect, despite the low values for eMd.Pm/B.Pm. Our qualitative examination of the periosteal surfaces of these animals suggests that any PTH effect on periosteal bone formation that ever occurred was no longer evident. The use of a ten day fluorochrome interlabel time period that is more appropriate for studying the cancellous and endocortical surfaces than the periosteal surface, may also have limited the ability to properly study periosteal bone formation [99].

Cortical area and thickness declined by six–nine months after OVX [105]. Both cortical area and thickness were better with anti-resorptive monotherapy [106] and, particularly, with treatments that combined PTH [64,90–92] with anti-resorptives, no matter the order of administration. Total area was not affected at any time, perhaps providing further evidence of a stable periosteum. Therefore, one can imply that the greater cortical area and thickness were due to extra bone at the endocortical surface, whether through anti-resorptive activity or PTH-stimulated deposition of lamellar bone. Cortical area and thickness, that are only indirect measures of the endocortical lamellar bone deposited during PTH therapy, were also influenced by inter-animal variation and to a smaller extent by variation in the location of the specific sections analyzed, accounting for their greater variability than the direct measurement of the endocortical lamellar bone itself. Greater cortical bone area and thickness were associated with better bone strength [60].

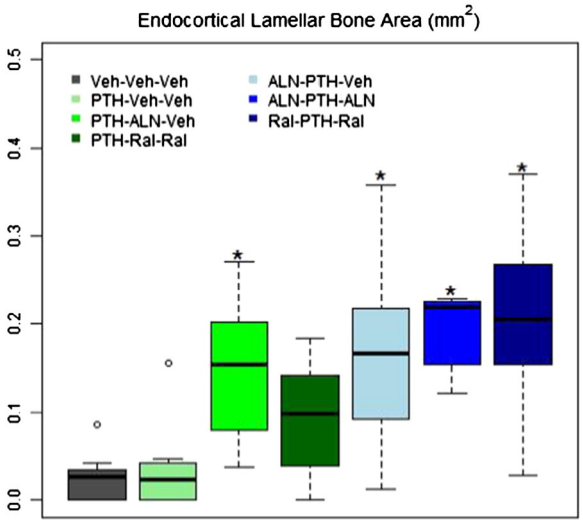

Fig. 4. Endocortical lamellar bone area at end of study. Boxes are as described in Fig. 1b. Increased lamellar bone area was observed only in groups that received both PTH and either pre- or post-PTH anti-resorptive treatment. Without such treatment, by the end of study, endocortical lamellar bone disappeared completely after PTH cessation. Three months without anti-resorptive treatment allowed some loss. Measurements were only obtained for the groups that received PTH at some point during the course of treatment and the Veh–Veh–Veh group. No data were collected (and no bars are shown) for the Sham, Aln–Aln–Aln, Ral–Ral–Ral, or Aln–Veh–Aln group.

Traditional monotherapies, such as continuous alendronate, continuous raloxifene, and fifteen weeks of PTH followed by no additional treatment, had little or no effect on cortical bone, despite the fact that they had a positive effect on trabecular bone in the same rats [75]. This strongly indicates that cortical bone in rats is less sensitive to traditional monotherapy than trabecular bone. It may also indicate that, in humans, when sites that are predominantly cortical, such as the proximal femur "respond" to traditional monotherapy, trabecular bone in the measurement field may be responsible for most of the response. We also found that only sequential polytherapy involving agents of complementary tissue level mechanisms of action caused a cortical bone response. This may indicate that sequential polytherapies are likely to be more effective than traditional monotherapy on bone sites in humans that are composed mainly of cortical bone.

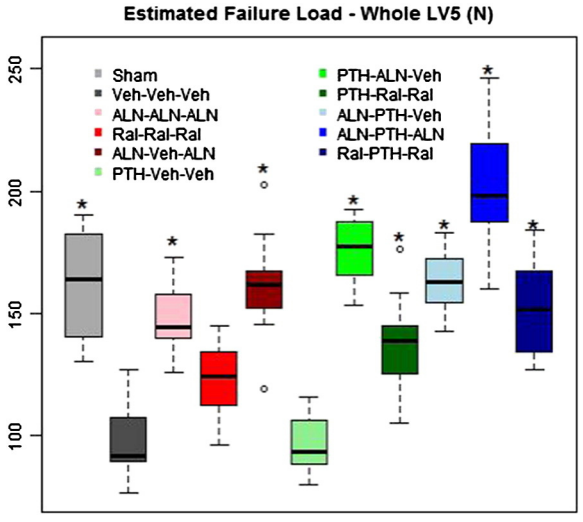

Fig. 5. Estimated failure load at end of study. Boxes are as described in Fig. 1b. Reduced estimated failure load was observed in OVX rats by the end of study. All groups except PTH–Veh–Veh and Ral–Ral–Ral, had better estimated failure load than OVX rats. These values were in the range of Sham rats.

The Aln "holiday" group (Aln–Veh–Aln) was generally among the best performing for maximum load, cortical thickness, and cortical area by the end of the experiment. These data may indicate that intermittent bisphosphonate therapy, that contains short "holidays" in which a relatively small amount of time is allowed for the effect of bone-retained bisphosphonate to abate before treatment resumes, could be as effective as continuous treatment for cortical bone. However, this positive finding may also be limited to the cortical bone of rats that has minimal Haversian remodeling, as lumbar vertebral body compression strength is lower, despite the persistence of higher BMD, in these same rats [75]. Discontinuation of Aln in humans is associated with increases in remodeling rate and declines in hip BMD that are apparent within 6–12 months of stopping treatment [107].

The degree of bone mineralization (DBM) [108] was significantly better in most treated groups than in untreated OVX rats, particularly those evaluated closer to the end of study. This probably indicates the success of anti-resorptive therapy that slows the turnover rate, resulting in an increase in the mean age of bone [109,110] without affecting secondary mineralization rate [111]. However, in a multiple regression analysis that also incorporated cortical area and cortical thickness, DBM was not an independent predictor of bone strength. Our FEM model, that did not consider DBM, "under-predicted" bone strength in the strongest bones that received both anti-resorptive and anabolic treatments. We conclude that a bone quality parameter other than DBM, that is not included in the FEM, may be responsible for the under-prediction.

Treatment did not affect IDI, an endpoint that assesses the resistance of bone tissue to directly applied force in tiny areas [112]. Furthermore, neither IDI nor AED values were correlated to maximum load. When used in live humans, this technique has had some success at identifying osteoporotic persons [80]. In animal studies, these endpoints appear to correlate to mechanical properties of bone [81–84,113]. We conclude that indentation properties of proximal femoral cortical bone were not affected by any treatment sequences applied here.

In this study, both pre-PTH and post-PTH anti-resorptive therapy reduced the rate of removal of PTH-induced endocortical lamellar bone. We used alendronate, a bisphosphonate, as our anti-resorptive. Bisphosphonates, unlike RANK Ligand antibodies, are retained in mineralized bone tissue with a multi-year half-life [114]. The release of retained bisphosphonate principally from trabecular bone tissue by osteoclastic resorption results in a gradual [16], rather than an abrupt [115], loss of anti-resorptive efficacy following treatment discontinuation. It seems likely that using a RANK Ligand antibody as an anti-resorptive during sequential therapy would be efficacious for preserving endocortical lamellar bone only during post-PTH treatment.

This pre-clinical study of rat cortical bone had multiple strengths. We studied clinical treatment sequences of bone active agents, measuring both non-destructive surrogate measures of cortical bone strength and bone strength itself. We used ninety-day treatment periods, approximately two remodeling periods in mature adult rats, that may represent up to 18 months in humans [104]. We evaluated treatments, such as monotherapy with a bisphosphonate, raloxifene, and PTH, for which clinical fracture risk reduction data exist. We measured surrogate bone strength endpoints in both the approved monotherapies, and other sequences of treatment for which clinical fracture risk data have not yet been collected, to enable predictions about which could offer improved fracture risk reduction compared to traditional monotherapy.

However, there were also a number of weaknesses. Rats, unlike humans, lack ambient Haversian remodeling of cortical bone [104], meaning that any changes in bone strength likely reflect changes in bone formation and resorption at the endocortical surface with a small contribution from the periosteal surface that might not reflect what would happen in humans. Since we began treatment at eight weeks post-OVX, a time when OVX-related bone loss was still ongoing, the findings may be best applied to women who are still losing bone after menopause. The dosing regimen of raloxifene that showed good efficacy in past work [22,55] was less frequent than that known to produce the

maximum possible effect of raloxifene on prevention of OVX-induced bone loss [3].

Conclusions

We studied cortical bone in both traditional monotherapy and sequential therapies with approved agents for human osteoporosis that operate through complementary tissue level mechanisms of action, during three consecutive three month treatment periods. We measured bone strength and several surrogate measures for bone strength in the central tibia on necropsy samples. Sequential therapy that involved an anabolic agent showed the best improvements in cortical bone strength. Anti-resorptive therapy, either preceding or following the anabolic agent, was required to maintain gains attributable to an anabolic agent.

Acknowledgments

This work was funded by National Institutes of Health Grants Nos. R01 AR043052 and K24 AR-048841, 1 P50 AR063043, and P50 AR060752NIH to NEL, the endowment for aging research at UC Davis to NEL, and the Center for Musculoskeletal Health at UC Davis. The sponsor played no role in this manuscript.

Appendix A. Supplementary data

Supplementary data to this article can be found online at http://dx.doi.org/10.1016/j.bone.2014.04.033.

References

[1] Salomon JA, Wang H, Freeman MK, Vos T, Flaxman AD, Lopez AD, et al. Healthy life expectancy for 187 countries, 1990–2010: a systematic analysis for the Global Burden Disease Study 2010. Lancet 2012;380(9859):2144–62. http://dx.doi.org/10.1016/S0140-6736(12)61690-0.
[2] Wang H, Dwyer-Lindgren L, Lofgren KT, Rajaratnam JK, Marcus JR, Levin-Rector A, et al. Age-specific and sex-specific mortality in 187 countries, 1970–2010: a systematic analysis for the Global Burden of Disease Study 2010. Lancet 2012;380(9859):2071–94. http://dx.doi.org/10.1016/S0140-6736(12)61719-X.
[3] Evans GL, Bryant HU, Magee DE, Turner RT. Raloxifene inhibits bone turnover and prevents further cancellous bone loss in adult ovariectomized rats with established osteopenia. Endocrinology 1996;137:4139–44.
[4] Ominsky MS, Li X, Asuncion FJ, Barrero M, Warmington KS, Dwyer D, et al. RANKL inhibition with osteoprotegerin increases bone strength by improving cortical and trabecular bone architecture in ovariectomized rats. J Bone Miner Res 2008;23:672–82. http://dx.doi.org/10.1359/jbmr.080109.
[5] Seedor JG, Quartuccio HA, Thompson DD. The bisphosphonate alendronate (MK-217) inhibits bone loss due to ovariectomy in rats. J Bone Miner Res 1991;6:339–46.
[6] Allen MR, Iwata K, Sato M, Burr DB. Raloxifene enhances vertebral mechanical properties independent of bone density. Bone 2006;39:1130–5.
[7] Black DM, Cummings SR, Karpf DB, Cauley JA, Thompson DE, Nevitt MC, et al. Randomised trial of effect of alendronate on risk of fracture in women with existing vertebral fractures. Fracture Intervention Trial Research Group. Lancet 1996;348(9041):1535–41.
[8] Cummings SR, Karpf DB, Harris F, Genant HK, Ensrud K, LaCroix AZ, et al. Improvement in spine bone density and reduction in risk of vertebral fractures during treatment with antiresorptive drugs. Am J Med 2002;112(4):281–9.
[9] Ettinger B, Black DM, Mitlak BH, Knickerbocker RK, Nickelsen T, Genant HK, et al. Reduction of vertebral fracture risk in postmenopausal women with osteoporosis treated with raloxifene: results from a 3-year randomized clinical trial. Multiple Outcomes of Raloxifene Evaluation (MORE) Investigators. JAMA 1999;282(7):637–45.
[10] Harrington JT, Ste-Marie LG, Brandi ML, Civitelli R, Fardellone P, Grauer A, et al. Risedronate rapidly reduces the risk for nonvertebral fractures in women with postmenopausal osteoporosis. Calcif Tissue Int 2004;74(2):129–35.
[11] Harris ST, Watts NB, Genant HK, McKeever CD, Hangartner T, Keller M, et al. Effects of risedronate treatment on vertebral and nonvertebral fractures in women with postmenopausal osteoporosis: a randomized controlled trial. Vertebral Efficacy With Risedronate Therapy (VERT) Study Group. JAMA 1999;282(14):1344–52.
[12] Liberman UA, Weiss SR, Broll J, Minne HW, Quan H, Bell NH, et al. Effect of oral alendronate on bone mineral density and the incidence of fractures in postmenopausal osteoporosis. The Alendronate Phase III Osteoporosis Treatment Study Group. N Engl J Med 1995;333(22):1437–43.
[13] Neer RM, Arnaud CD, Zanchetta JR, Prince R, Gaich GA, Reginster JY, et al. Effect of parathyroid hormone (1–34) on fractures and bone mineral density in postmenopausal women with osteoporosis. N Engl J Med 2001;344(19):1434–41.
[14] Cummings SR, San Martin J, McClung MR, Siris ES, Eastell R, Reid IR, et al. Denosumab for prevention of fractures in postmenopausal women with osteoporosis. N Engl J Med 2009;361(8):756–65.
[15] Black DM, Delmas PD, Eastell R, Reid IR, Boonen S, Cauley JA, et al. Once-yearly zoledronic acid for treatment of postmenopausal osteoporosis. N Engl J Med 2007;356(18):1809–22.
[16] Black DM, Schwartz AV, Ensrud KE, Cauley JA, Levis S, Quandt SA, et al. Effects of continuing or stopping alendronate after 5 years of treatment: the Fracture Intervention Trial Long-term Extension (FLEX): a randomized trial. JAMA 2006;296(24):2927–38.
[17] Kimmel DB, Bozzato RP, Kronis KA, Coble T, Sindrey D, Kwong P, et al. The effect of recombinant human (1–84) or synthetic human (1–34) parathyroid hormone on the skeleton of adult osteopenic ovariectomized rats. Endocrinology 1993;132:1577–84.
[18] Wronski TJ, Yen CF, Qi H, Dann LM. Parathyroid hormone is more effective than estrogen or bisphosphonates for restoration of lost bone mass in ovariectomized rats. Endocrinology 1993;132:823–31.
[19] Arita S, Ikeda S, Sakai A, Okimoto N, Akahoshi S, Nagashima M, et al. Human parathyroid hormone (1–34) increases mass and structure of the cortical shell, with resultant increase in lumbar bone strength, in ovariectomized rats. J Bone Miner Metab 2004;22:530–40.
[20] Han SL, Wan SL. Effect of teriparatide on bone mineral density and fracture in postmenopausal osteoporosis: meta-analysis of randomised controlled trials. Int J Clin Pract 2012;66(2):199–209.
[21] Murad MH, Drake MT, Mullan RJ, Mauck KF, Stuart LM, Lane MA, et al. Clinical review. Comparative effectiveness of drug treatments to prevent fragility fractures: a systematic review and network meta-analysis. J Clin Endocrinol Metab 2012;97(6):1871–80. http://dx.doi.org/10.1210/jc.2011-3060.
[22] Cheng Z, Yao W, Zimmermann EA, Busse C, Ritchie RO, Lane NE. Prolonged treatments with antiresorptive agents and PTH have different effects on bone strength and the degree of mineralization in old estrogen-deficient osteoporotic rats. J Bone Miner Res 2009;24(2):209–20. http://dx.doi.org/10.1359/jbmr.81005.
[23] Neer RM, Arnaud CD, Zanchetta JR, Prince R, Gaich GA, Reginster JY, et al. Effect of parathyroid hormone (1–34) on fractures and bone mineral density in postmenopausal women with osteoporosis. N Engl J Med 2001;344:1434–41.
[24] Capriani C, Irani D, Bilezikian JP. Safety of osteoanabolic therapy: a decade of experience. J Bone Miner Res 2012;27(12):2419–28. http://dx.doi.org/10.1002/jbmr.1800.
[25] Turner RT, Lotinun S, Hefferan TE, Morey-Holton E. Disuse in adult male rats attenuates the bone anabolic response to a therapeutic dose of parathyroid hormone. J Appl Physiol 2006;101:881–6.
[26] Kneissel M, Boyde A, Gasser JA. Bone tissue and its mineralization in aged estrogen-depleted rats after long-term intermittent treatment with parathyroid hormone (PTH) analog SDZ PTS 893 or human PTH (1–34). Bone 2001;28:237–50.
[27] Misof BM, Roschger P, Cosman F, Kurland ES, Tesch W, Messmer P, et al. Effects of intermittent parathyroid hormone administration on bone mineralization density in iliac crest biopsies from patients with osteoporosis: a paired study before and after treatment. J Clin Endocrinol Metab 2003;88:1150–6.
[28] Sarkar S, Mitlak BH, Wong M, Stock JL, Black DM, Harper KD. Relationships between bone mineral density and incident vertebral fracture risk with raloxifene therapy. J Bone Miner Res 2002;17(1):1–10.
[29] Bala Y, Farlay D, Chapurlat RD, Boivin G. Modifications of bone material properties in postmenopausal osteoporotic women long-term treated with alendronate. Eur J Endocrinol 2011;165:647–55. http://dx.doi.org/10.1530/EJE-11-0333.
[30] Boivin GY, Meunier PJ. Changes in bone remodeling rate influence the degree of mineralization of bone. Connect Tissue Res 2002;43:535–7.
[31] Boivin GY, Chavassieux PM, Santora AC, Yates J, Meunier PJ. Alendronate increases bone strength by increasing the mean degree of mineralization of bone tissue in osteoporotic women. Bone 2000;27(5):687–94.
[32] Borah B, Dufresne TE, Ritman EL, Jorgensen SM, Liu S, Chmielewski PA, et al. Long-term risedronate treatment normalizes mineralization and continues to preserve trabecular architecture: sequential triple biopsy studies with micro-computed tomography. Bone 2006;39(2):345–52.
[33] Borah B, Ritman EL, Dufresne TE, Jorgensen SM, Liu S, Sacha J, et al. The effect of risedronate on bone mineralization as measured by micro-computed tomography with synchrotron radiation: correlation to histomorphometric indices of turnover. Bone 2005;37(1):1–9.
[34] Burr DB, Miller L, Grynpas M, Li J, Boyde A, Mashiba T, et al. Tissue mineralization is increased following 1-year treatment with high doses of bisphosphonates in dogs. Bone 2003;33(6):960–9.
[35] Roschger P, Rinnerthaler S, Yates J, Rodan GA, Fratzl P, Klaushofer K. Alendronate increases degree and uniformity of mineralization in cancellous bone and decreases the porosity in cortical bone of osteoporotic women. Bone 2001;29(2):185–91.
[36] Zoehrer R, Roschger P, Paschalis EP, Hofstaetter JG, Durchschlag E, Fratzl P, et al. Effects of 3- and 5-year treatment with risedronate on bone mineralization density distribution in triple biopsies of the iliac crest in postmenopausal women. J Bone Miner Res 2006;21(7):1106–12.
[37] Eriksen EF, Melsen F, Sod E, Barton I, Chines A. Effects of long-term risedronate on bone quality and bone turnover in women with postmenopausal osteoporosis. Bone 2002;31:620–5.
[38] Iwamoto J, Matsumoto H, Takeda T, Sato Y, Xu E, Yeh JK. Effects of alendronate and alfacalcidol on the femoral bone mass and bone strength in orchidectomized rats. Chin J Physiol 2008;51:331–7.
[39] Mashiba T, Hirano T, Turner CH, Forwood MR, Johnston CC, Burr DB. Suppressed bone turnover by bisphosphonates increases microdamage accumulation and reduces some biomechanical properties in dog rib. J Bone Miner Res 2000;15:613–20.

[40] Lafage MH, Balena R, Battle MA, Shea M, Seedor JG, Klein H, et al. Comparison of alendronate and sodium fluoride effects on cancellous and cortical bone in minipigs. J Clin Invest 1995;95:2127–33.
[41] Hofstaetter JG, Wang J, Hofstaetter SG, Glimcher MJ. The effects of high-dose, long-term alendronate treatment on microarchitecture and bone mineral density of compact and trabecular bone in the proximal femur of adult male rabbits. Arch Orthop Trauma Surg 2010;130:937–44. http://dx.doi.org/10.1007/s00402-010-1116-1.
[42] Hyldstrup L, Jørgensen JT, Sørensen TK, Baeksgaard L. Response of cortical bone to antiresorptive treatment. Calcif Tissue Int 2001;68:135–9.
[43] Borah B, Dufresne T, Nurre J, Phipps R, Chmielewski P, Wagner L, et al. Risedronate reduces intracortical porosity in women with osteoporosis. J Bone Miner Res 2010;25:41–7. http://dx.doi.org/10.1359/jbmr.090711.
[44] Bala Y, Chapurlat R, Cheung AM, Felsenberg D, LaRoche M, Morris E, et al. Risedronate slows or partly reverses cortical and trabecular microarchitectural deterioration in postmenopausal women. J Bone Miner Res 2014;29:380–8. http://dx.doi.org/10.1002/jbmr.2101.
[45] Chavassieux P, Meunier PJ, Roux JP, Portero-Muzy N, Pierre M, Chapurlat R. Bone histomorphometry of transiliac paired bone biopsies after 6 or 12 months of treatment with oral strontium ranelate in 387 osteoporotic women: randomized comparison to alendronate. J Bone Miner Res 2014;29:618–28. http://dx.doi.org/10.1002/jbmr.2074.
[46] Misof BM, Patsch JM, Roschger P, Muschitz C, Gamsjaeger S, Paschalis EP, et al. Intravenous treatment with ibandronate normalizes bone matrix mineralization and reduces cortical porosity after two years in male osteoporosis: a paired biopsy study. J Bone Miner Res 2014;29:440–9. http://dx.doi.org/10.1002/jbmr.2035.
[47] Gasser JA, Ingold P, Venturiere A, Shen V, Green JR. Long-term protective effects of zoledronic acid on cancellous and cortical bone in the ovariectomized rat. J Bone Miner Res 2008;23:544–51.
[48] Seeman E, Delmas PD, Hanley DA, Sellmeyer D, Cheung AM, Shane E, et al. Microarchitectural deterioration of cortical and trabecular bone: differing effects of denosumab and alendronate. J Bone Miner Res 2010;25:1886–94. http://dx.doi.org/10.1002/jbmr.81.
[49] Burghardt AJ, Kazakia GJ, Sode M, de Papp AE, Link TM, Majumdar S. A longitudinal HR-pQCT study of alendronate treatment in postmenopausal women with low bone density: relations among density, cortical and trabecular microarchitecture, biomechanics, and bone turnover. J Bone Miner Res 2010;25:2558–71. http://dx.doi.org/10.1002/jbmr.157.
[50] Wronski TJ, Dann LM, Scott KS, Crooke LR. Endocrine and pharmacological suppressors of bone turnover protect against osteopenia in ovariectomized rats. Endocrinology 1989;125:810–6.
[51] Black DM, Thompson DE, Bauer DC, Ensrud K, Musliner T, Hochberg MC, et al. Fracture risk reduction with alendronate in women with osteoporosis: the Fracture Intervention Trial. FIT Research Group. J Clin Endocrinol Metab 2000;85(11):4118–24.
[52] Boivin G, Lips P, Ott SM, Harper KD, Sarkar S, Pinette KV, et al. Contribution of raloxifene and calcium and vitamin D3 supplementation to the increase of the degree of mineralization of bone in postmenopausal women. J Clin Endocrinol Metab 2003;88(9):4199–205.
[53] Hirano T, Turner CH, Forwood MR, Johnston CC, Burr DB. Does suppression of bone turnover impair mechanical properties by allowing microdamage accumulation? Bone 2000;27(1):13–20.
[54] Shahnazari M, Yao W, Dai W, Wang B, Ionova-Martin SS, Ritchie RO, et al. Higher doses of bisphosphonates further improve bone mass, architecture, and strength but not the tissue material properties in aged rats. Bone 2010;46(5):1267–74. http://dx.doi.org/10.1016/j.bone.2009.11.019.
[55] Yao W, Cheng Z, Koester KJ, Ager JW, Balooch M, Pham A, et al. The degree of bone mineralization is maintained with single intravenous bisphosphonates in aged estrogen-deficient rats and is a strong predictor of bone strength. Bone 2007;41(5):804–12.
[56] Ma YL, Zeng QQ, Chiang AY, Burr DB, Li J, Dobnig H, et al. Effects of teriparatide on cortical histomorphometric variables in postmenopausal women with or without prior alendronate treatment. Bone 2014;59:139–47. http://dx.doi.org/10.1016/j.bone.2013.11.011.
[57] Fox J, Miller MA, Newman MK, Recker RR, Turner CH, Smith SY. Effects of daily treatment with parathyroid hormone 1–84 for 16 months on density, architecture and biomechanical properties of cortical bone in adult ovariectomized rhesus monkeys. Bone 2007;41:321–30.
[58] Mashiba T, Burr DB, Turner CH, Sato M, Cain RL, Hock JM. Effects of human parathyroid hormone (1–34), LY333334, on bone mass, remodeling, and mechanical properties of cortical bone during the first remodeling cycle in rabbits. Bone 2001;28:538–47.
[59] Ma YL, Marin F, Stepan JJ, Ish-Shalom S, Möricke R, Hawkins F, et al. Comparative effects of teriparatide and strontium ranelate in the periosteum of iliac crest biopsies in postmenopausal women with osteoporosis. Bone 2011;48:972–8. http://dx.doi.org/10.1016/j.bone.2011.01.012.
[60] Gafni RI, Brahim JS, Andreopoulou P, Bhattacharyya N, Kelly MH, Brillante BA, et al. Daily parathyroid hormone 1–34 replacement therapy for hypoparathyroidism induces marked changes in bone turnover and structure. J Bone Miner Res 2012;27:1811–20. http://dx.doi.org/10.1002/jbmr.1627.
[61] Wronski TJ, Yen CF. Anabolic effects of parathyroid hormone on cortical bone in ovariectomized rats. Bone 1994;15(1):51–8.
[62] Fox J, Miller MA, Recker RR, Turner CH, Smith SY. Effects of treatment of ovariectomized adult rhesus monkeys with PTH (1–84) for 16 months on trabecular and cortical bone structure and biomechanical properties of the proximal femur. Calcif Tissue Int 2007;81:53–63.
[63] Recker RR, Bare SP, Smith SY, Varela A, Miller MA, Morris SA, et al. Cancellous and cortical bone architecture and turnover at the iliac crest of postmenopausal osteoporotic women treated with parathyroid hormone 1–84. Bone 2009;44:113–9. http://dx.doi.org/10.1016/j.bone.2008.09.019.
[64] Baumann BD, Wronski TJ. Response of cortical bone to antiresorptive agents and parathyroid hormone in aged ovariectomized rats. Bone 1995;16:247–53.
[65] Sato M, Westmore M, Ma YL, Schmidt A, Zeng QQ, Glass EV, et al. Teriparatide [PTH(1–34)] strengthens the proximal femur of ovariectomized nonhuman primates despite increasing porosity. J Bone Miner Res 2004;19:623–9.
[66] Brouwers JE, van Rietbergen B, Huiskes R, Ito K. Effects of PTH treatment on tibial bone of ovariectomized rats assessed by in vivo micro-CT. Osteoporos Int 2009;20:1823–35. http://dx.doi.org/10.1007/s00198-009-0882-5.
[67] Sugiyama T, Saxon LK, Zaman G, Moustafa A, Sunters A, Price JS, et al. Mechanical loading enhances the anabolic effects of intermittent parathyroid hormone (1–34) on trabecular and cortical bone in mice. Bone 2008;43:238–310. http://dx.doi.org/10.1016/j.bone.2008.04.012.
[68] Black DM, Bilezikian JP, Ensrud KE, Greenspan SL, Palermo L, Hue T, et al. One year of alendronate after one year of parathyroid hormone (1–84) for osteoporosis. N Engl J Med 2005;353(6):555–65.
[69] Cosman F, Nieves JW, Zion M, Barbuto N, Lindsay R. Effect of prior and ongoing raloxifene therapy on response to PTH and maintenance of BMD after PTH therapy. Osteoporos Int 2008;19(4):529–35.
[70] Ettinger B, San Martin J, Crans G, Pavo I. Differential effects of teriparatide on BMD after treatment with raloxifene or alendronate. J Bone Miner Res 2004;19(5):745–51.
[71] Greenspan SL, Beck TJ, Resnick NM, Bhattacharya R, Parker RA. Effect of hormone replacement, alendronate, or combination therapy on hip structural geometry: a 3-year, double-blind, placebo-controlled clinical trial. J Bone Miner Res 2005;20(9):1525–32.
[72] Shahnazari M, Yao W, Wang B, Panganiban B, Ritchie RO, Hagar Y, et al. Differential maintenance of cortical and cancellous bone strength following discontinuation of bone-active agents. J Bone Miner Res 2011;26(3):569–81. http://dx.doi.org/10.1002/jbmr.249.
[73] Agholme F, Macias B, Hamang M, Lucchesi J, Adrian MD, Kuhstoss S, et al. Efficacy of a sclerostin antibody compared to a low dose of PTH on metaphyseal bone healing. J Orthop Res 2014;32:471–6. http://dx.doi.org/10.1002/jor.22525.
[74] Komatsu DE, Brune KA, Liu H, Schmidt AL, Han B, Zeng QQ, et al. Longitudinal in vivo analysis of the region-specific efficacy of parathyroid hormone in a rat cortical defect model. Endocrinology 2009;150:1570–9. http://dx.doi.org/10.1210/en.2008-0814.
[75] Amugongo SK, Yao W, Jia J, Lay YE, Dai W, Jiang L, et al. Effects of sequential osteoporosis treatments on trabecular bone mass and strength in rats with low bone mass. Osteoporos Int 2014;25(6):1735–50.
[76] Bentolila V, Boyce TM, Fyhrie DP, Drumb R, Skerry TM, Schaffler MB. Intracortical remodeling in adult rat long bones after fatigue loading. Bone 1998;23:275–81.
[77] Balooch G, Yao W, Ager JW, Balooch M, Nalla RK, Porter AE, et al. The aminobisphosphonate risedronate preserves localized mineral and material properties of bone in the presence of glucocorticoids. Arthritis Rheum 2007;56:3726–37.
[78] Ritchie RO, Koester KJ, Ionova S, Yao W, Lane NE, Ager III JW. Measurement of the toughness of bone: a tutorial with special reference to small animal studies. Bone 2008;43(5):798–812.
[79] Dempster DW, Compston JE, Drezner MK, Glorieux FH, Kanis JA, Malluche H, et al. Standardized nomenclature, symbols, and units for bone histomorphometry: a 2012 update of the report of the ASBMR Histomorphometry Nomenclature Committee. J Bone Miner Res 2013;28(1):2–17. http://dx.doi.org/10.1002/jbmr.1805.
[80] Diez-Perez A, Guerri R, Nogues X, Caceres E, Pena MJ, Mellibovsky L, et al. Microindentation for in vivo measurement of bone tissue mechanical properties in humans. J Bone Miner Res 2010;25(8):1877–85. http://dx.doi.org/10.1002/jbmr.73.
[81] Gallant MA, Brown DM, Organ JM, Allen MR, Burr DB. Reference-point indentation correlates with bone toughness assessed using whole-bone traditional mechanical testing. Bone 2013;53(1):301–5. http://dx.doi.org/10.1016/j.bone.2012.12.015 [Epub 2012 Dec 27].
[82] Rasoulian R, Raeisi Najafi A, Chittenden M, Jasiuk I. Reference point indentation study of age-related changes in porcine femoral cortical bone. J Biomech 2013;46:1689–96. http://dx.doi.org/10.1016/j.jbiomech.2013.04.003.
[83] Aref M, Gallant MA, Organ JM, Wallace JM, Newman CL, Burr DB, et al. In vivo reference point indentation reveals positive effects of raloxifene on mechanical properties following 6 months of treatment in skeletally mature beagle dogs. Bone 2013;56:449–53. http://dx.doi.org/10.1016/j.bone.2013.07.009.
[84] Milovanovic P, Rakocevic Z, Djonic D, Zivkovic V, Hahn M, Nikolic S, et al. Nanostructural, compositional and micro-architectural signs of cortical bone fragility at the superolateral femoral neck in elderly hip fracture patients vs. healthy aged controls. Exp Gerontol 2014;55C:19–28. http://dx.doi.org/10.1016/j.exger.2014.03.001 [Epub ahead of print].
[85] Ladd AJ, Kinney JH, Haupt DL, Goldstein SA. Finite-element modeling of trabecular bone: comparison with mechanical testing and determination of tissue modulus. J Orthop Res 1998;16:622–8.
[86] van Rietbergen B, Weinans H, Huiskes R, Odgaard A. A new method to determine trabecular bone elastic properties and loading using micromechanical finite-element models. J Biomech 1995;28:69–81.
[87] Eswaran SK, Gupta A, Adams MF, Keaveny TM. Cortical and trabecular load sharing in the human vertebral body. J Bone Miner Res 2006;21:307–14.
[88] Ulrich D, Rietbergen B, Laib A, Ruegsegger P. Mechanical analysis of bone and its microarchitecture based on in vivo voxel images. Technol Health Care 1998;6:421–7.
[89] Rhee Y, Hur JH, Won YY, Lim SK, Beak MH, Cui WQ, et al. Assessment of bone quality using finite element analysis based upon micro-CT images. Clin Orthop Surg 2009;1:40–7. http://dx.doi.org/10.4055/cios.2009.1.1.40.

[90] Ejersted C, Andreassen TT, Oxlund H, Jørgensen PH, Bak B, Häggblad J, et al. Human parathyroid hormone (1–34) and (1–84) increase the mechanical strength and thickness of cortical bone in rats. J Bone Miner Res 1993;8(9):1097–101.
[91] Mosekilde L, Danielsen CC, Sogaard CH, McOsker JE, Wronski TJ. The anabolic effects of parathyroid hormone on cortical bone mass, dimensions and strength—assessed in a sexually mature, ovariectomized rat model. Bone 1995;16(2):223–30.
[92] Ejersted C, Oxlund H, Andreassen TT. Bisphosphonate maintains parathyroid hormone (1–34)-induced cortical bone mass and mechanical strength in old rats. Calcif Tissue Int 1998;62(4):316–22.
[93] Zanchetta JR, Bogado CE, Ferretti JL, Wang O, Wilson MG, Sato M, et al. Effects of teriparatide [recombinant human parathyroid hormone (1–34)] on cortical bone in postmenopausal women with osteoporosis. J Bone Miner Res 2003;18:539–43.
[94] Lindsay R, Zhou H, Cosman F, Nieves J, Dempster DW, Hodsman AB. Effects of a one-month treatment with PTH (1–34) on bone formation on cancellous, endocortical, and periosteal surfaces of the human ilium. J Bone Miner Res 2007;22:495–502.
[95] Ma YL, Zeng Q, Donley DW, Ste-Marie LG, Gallagher JC, Dalsky GP, et al. Teriparatide increases bone formation in modeling and remodeling osteons and enhances IGF-II immunoreactivity in postmenopausal women with osteoporosis. J Bone Miner Res 2006;21:855–64.
[96] Lindsay R, Cosman F, Zhou H, Bostrom MP, Shen VW, Cruz JD, et al. A novel tetracycline labeling schedule for longitudinal evaluation of the short-term effects of anabolic therapy with a single iliac crest bone biopsy: early actions of teriparatide. J Bone Miner Res 2006;21:366–73.
[97] Arlot M, Meunier PJ, Boivin G, Haddock L, Tamayo J, Correa-Rotter R, et al. Differential effects of teriparatide and alendronate on bone remodeling in postmenopausal women assessed by histomorphometric parameters. J Bone Miner Res 2005;20:1244–53.
[98] Recker RR, Marin F, Ish-Shalom S, Moricke R, Hawkins F, Kapetanos G, et al. Comparative effects of teriparatide and strontium ranelate on bone biopsies and biochemical markers of bone turnover in postmenopausal women with osteoporosis. J Bone Miner Res 2009;24:1358–68.
[99] Sibonga JD, Iwaniec UT, Shogren KL, Rosen CJ, Turner RT. Effects of parathyroid hormone (1–34) on tibia in an adult rat model for chronic alcohol abuse. Bone 2007;40:1013–20.
[100] Engelke K, Stampa B, Timm W, Dardzinski B, de Papp AE, Genant HK, et al. Short-term in vivo precision of BMD and parameters of trabecular architecture at the distal forearm and tibia. Osteoporos Int 2012;23:2151–8. http://dx.doi.org/10.1007/s00198-011-1829-1. Epub 2011 Dec 6.
[101] MacNeil JA, Boyd SK. Improved reproducibility of high-resolution peripheral quantitative computed tomography for measurement of bone quality. Med Eng Phys 2008;30(6):792–9. http://dx.doi.org/10.1016/j.medengphy.2007.11.003. Epub 2008 Mar 4.
[102] Kazakia GJ, Hyun B, Burghardt AJ, Krug R, Newitt DC, de Papp AE, et al. In vivo determination of bone structure in postmenopausal women: a comparison of HR-pQCT and high-field MR imaging. J Bone Miner Res 2008;23:463–74.
[103] Kneissel M, Boyde A, Gasser JA. Bone tissue and its mineralization in aged estrogen-depleted rats after long-term intermittent treatment with parathyroid hormone (PTH) analog SDZ PTS 893 or human PTH (1–34). Bone 2001;28:237–50.
[104] Frost HM, Jee WSS. On the rat model of human osteopenias and osteoporoses. Bone Miner 1992;18:227–36.
[105] Danielsen CC, Mosekilde L, Svenstrup B. Cortical bone mass, composition, and mechanical properties in female rats in relation to age, long-term ovariectomy, and estrogen substitution. Calcif Tissue Int 1993;52:26–33.
[106] Fuchs RK, Shea M, Durski SL, Winters-Stone KM, Widrick J, Snow CM. Individual and combined effects of exercise and alendronate on bone mass and strength in ovariectomized rats. Bone 2007;41(2):290–6.
[107] Ensrud KE, Barrett-Connor EL, Schwartz A, Santora AC, Bauer DC, Suryawanshi S, et al. Randomized trial of effect of alendronate continuation versus discontinuation in women with low BMD: results from the Fracture Intervention Trial long-term extension. J Bone Miner Res 2004;19:1259–69.
[108] Burghardt AJ, Kazakia GJ, Laib A, Majumdar S. Quantitative assessment of bone tissue mineralization with polychromatic micro-computed tomography. Calcif Tissue Int 2008;83(2):129–38. http://dx.doi.org/10.1007/s00223-008-9158-x.
[109] Boivin G. Bone mineralization and mineral status. Therapie 2003;58(5):409–13.
[110] Mashiba T, Mori S, Burr DB, Komatsubara S, Cao Y, Manabe T, et al. The effects of suppressed bone remodeling by bisphosphonates on microdamage accumulation and degree of mineralization in the cortical bone of dog rib. J Bone Miner Metab 2005;23:36–42 [Suppl.].
[111] Fuchs RK, Faillace ME, Allen MR, Phipps RJ, Miller LM, Burr DB. Bisphosphonates do not alter the rate of secondary mineralization. Bone 2011;49(4):701–5. http://dx.doi.org/10.1016/j.bone.2011.05.009. Epub 2011 May 18.
[112] Hansma P, Turner P, Drake B, Yurtsev E, Proctor A, Mathews P, et al. The bone diagnostic instrument II: indentation distance increase. Rev Sci Instrum 2008;79(6):064303. http://dx.doi.org/10.1063/1.2937199.
[113] Hammond MA, Gallant MA, Burr DB, Wallace JM. Nanoscale changes in collagen are reflected in physical and mechanical properties of bone at the microscale in diabetic rats. Bone Nov 21 2013. http://dx.doi.org/10.1016/j.bone.2013.11.015 [pii: S8756-3282(13)00476-6].
[114] Khan SA, Kanis JA, Vasikaran S, Kline WF, Matuszewski BK, McCloskey EV, et al. Elimination and biochemical responses to intravenous alendronate in postmenopausal osteoporosis. J Bone Miner Res 1997;12:1700–7.
[115] Bone HG, Bolognese MA, Yuen CK, Kendler DL, Miller PD, Yang YC, et al. Effects of denosumab treatment and discontinuation on bone mineral density and bone turnover markers in postmenopausal women with low bone mass. J Clin Endocrinol Metab 2011;96:972–80. http://dx.doi.org/10.1210/jc.2010-1502.